Available online at www.sciencedirect.com
ScienceDirect
Biochimica et Biophysica Acta 1778 (2008) 334–341
Biochimica et Biophysica Acta BBA
www.elsevier.com/locate/bbamem

Site-directed mutagenesis investigation of coupling properties of metal ion transport by DCT1

Yaniv Nevo *

Department of Biochemistry, The George S. Wise Faculty of Life Sciences, Tel Aviv University, Tel Aviv 69978, Israel

Received 4 August 2007; received in revised form 20 September 2007; accepted 8 October 2007
Available online 16 October 2007

Abstract

DCT1 (NRAMP2, DMT1, slc11a2) is a member of the NRAMP family and functions as general metal ion transporter in mammals; defective DCT1 causes anemia. The driving force for metal ion transport is protonmotive force, where protons are transported in the same direction as metal ions. The stoichiometry between metal ion and proton varies under different conditions due to mechanistic proton slip. To better understand this phenomenon, we performed site-directed mutagenesis of DCT1 and analyzed the mutants by measurement of metal ion uptake activity and electrophysiology in *Xenopus laevis* oocytes. A single reciprocal mutation, I144F, between DCT1 and the homologous yeast transporter Smf1p located in putative transmembrane domain 2 abolished the metal ion transport activity of DCT1, significantly increased the slip currents, and generated sodium slip currents. A double mutation adding F227I in transmembrane domain 4 to I144F in transmembrane domain 2 restored the uptake activity of DCT1 and reduced the slip currents. These results demonstrate the importance of these regions in coupling of metal ions and protons as well as the possible proximity of I144 and F227 in the folded structure of DCT1.

Keywords: NRAMP; Metal ion; Proton; Coupling; Slip; Anemia

1. Introduction

Metal ions are vital life elements that participate in many metabolic processes in every living cell. However, at elevated levels these essential nutrients are toxic. Therefore, cells must maintain metal ion homeostasis. This is accomplished by highly regulated processes of uptake, storage, and secretion. In the last few years, it has become apparent that in organisms ranging from bacteria to man, the natural resistance-associated macrophage protein (NRAMP) family of metal ion transporters plays a major role in metal ion homeostasis [1–5], functioning as general metal ion transporters and transporting Mn^{2+}, Zn^{2+}, Cu^{2+}, Fe^{2+}, Cd^{2+}, Ni^{2+}, and Co^{2+} [6–10].

Most information regarding the function of these transporters is derived from studies of mammalian NRAMP2 (DCT1, DMT1, Slc11a2) and the yeast transporter SMF1 expressed in *Xenopus* oocytes [6–12]. Such studies demonstrated that DCT1 and Smf1p transport divalent metal ions and protons and that this process is driven by a proton gradient [9,11]. However, the transport of metal ions and protons is loosely coupled; the process exhibits variable stoichiometry. At pH 7 and membrane potentials of −90 mV to −30 mV, DCT1 transports one Fe^{2+} with one H^+. At high proton concentrations (pH 5.5), 10 H^+ are transported with each Fe^{2+} [9]. Moreover, at this low pH, with a reduction in membrane potential from +10 mV to −80 mV the number of H^+ transported for each Fe^{2+} increases from 3 to approximately 18 [11]. In DCT1, this phenomenon is termed metal ion-dependent proton slip [1,11,13]. In contrast, Smf1p exhibits metal ion-independent sodium slip through the proton-translocation pathway [11,14].

Recently, in an attempt to locate the transporter sites that mediate proton slip in DCT1, we created the mutation F227I (Fig. 1) in the putative transmembrane (TM) domain 4 (TM4) [10]. This mutation resulted in an increase of up to 14-fold in the ratio of transported metal ions to transported protons without any significant changes in metal ion transport activity and levels of transporter expression [10]. This finding suggests that proton slip is not a mechanistic necessity and supports the idea that proton slip confers a physiological advantage and was positively selected during the evolution of DCT1. However, the mechanism

* Tel.: +972 52 5349988; fax: +972 3 640 6018.
E-mail address: nevoyani@post.tau.ac.il.

0005-2736/$ - see front matter © 2007 Elsevier B.V. All rights reserved.
doi:10.1016/j.bbamem.2007.10.007

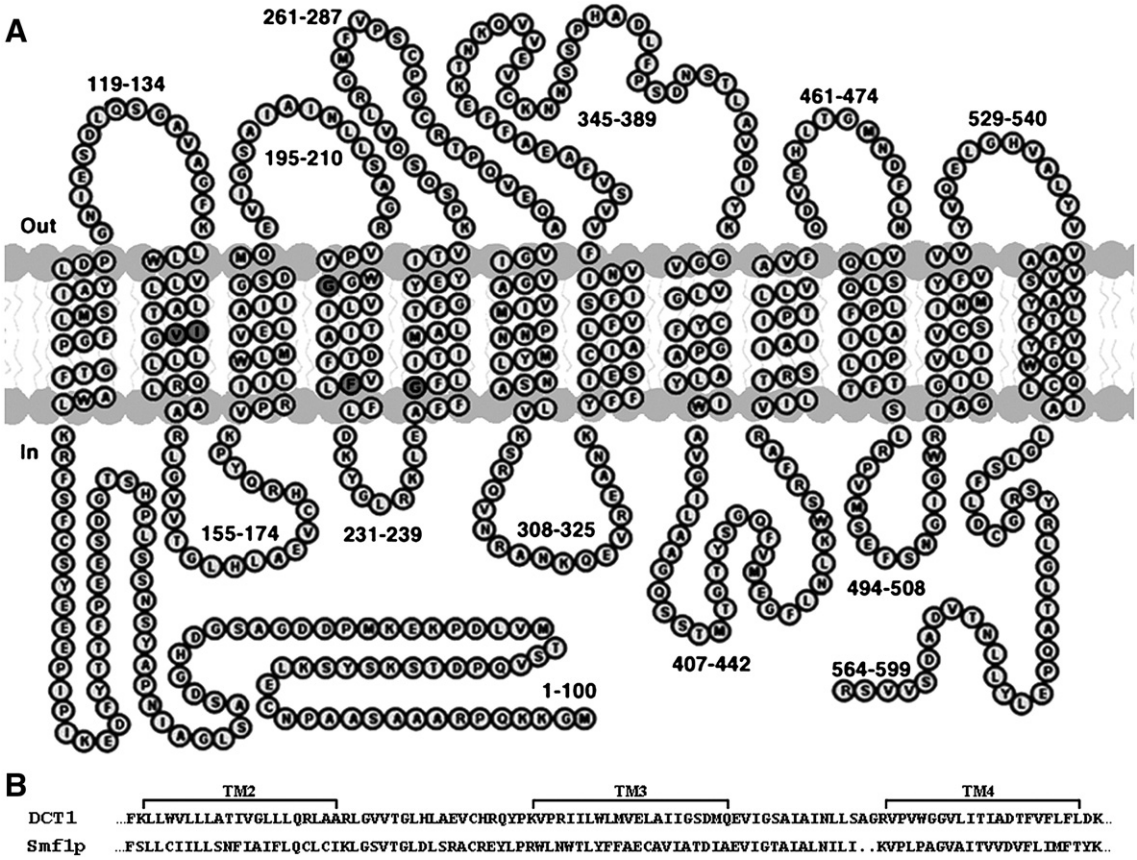

Fig. 1. Schematic representation of DCT1 (A). The predicted 12 transmembrane domains and individual intracellular (In) and extracellular (Out) segments are identified, along with their position within the primary sequence. The N- and C-termini are intracellular, and the loop between transmembrane domains 7 and 8 is extracellular. The G216R mutation in TM4 causes microcytic anemia in *mk/mk* mice and Belgrade rats [19–22]. (B) Alignment between DCT1 and Smf1p, from putative TM2 to TM4. The amino acid sequence of yeast Smf1p was obtained from ref. 6; the rat DCT1 (Nramp2) is from GenBank accession no. AF008439.

underlying this phenomenon is not well characterized, and the identity of the proton translocation pathway remains unknown.

DCT1 is thought to play a crucial role in iron absorption from the duodenum and in transport of iron released in the endosomes of many cell types at low pH [15–17]. There are compelling examples of the importance of DCT1. For example, *Slc11a2*$^{-/-}$ (*DCT1*$^{-/-}$) mice die within the first few days of life of severe systemic iron deficiency and consequent anemia [18]. Also, a single mutation in DCT1 (G216R) (Fig. 1) causes microcytic anemia in *mk* mice and *Belgrade* rats [19–22]. In humans, there are three known cases of severe microcytic anemia in patients with mutations in *DCT1*. The first two cases have been described in detail, together with the functional properties of the mutated DCT1 proteins expressed in yeast and cell lines [23–27]. Beaumont et al. reported the third case, a 10-year-old female patient [28]. This patient is a compound heterozygote for two novel mutations of *DCT1*. The first mutation is a 3-bp deletion (del GTG) in exon 5, leading to a V145 (V114) in-frame deletion in transmembrane domain 2 (TM2; Fig. 1), and the second mutation is a G to T substitution in exon 8 leading to replacement of G243V (G212V) in transmembrane domain 5 (TM5; Fig. 1) [28]. The effects of these two mutations (V145 deletion and G243V) on DCT1 function are unknown.

In this work, we investigated proton slip in DCT1 and report mutations that affect the uptake activity, metal ion-induced currents, ion binding, and specificity of DCT1. These mutations inform the structure and function of DCT1 and the deleterious effect of the in-frame deletion of V145 (V114) in the *DCT1* gene of an anemic patient.

2. Materials and methods

2.1. Site-Directed Mutagenesis of DCT1

Oligonucleotide-directed, site-specific mutagenesis was performed by overlapping nucleotides with the mutation using polymerase chain reaction (PCR) [29]. DCT1 cDNA was cloned into the pSPORT1 plasmid and used as a template for PCR mutagenesis. *Nde*I and *Spe*I restriction sites were introduced at positions 145 and 1719 of the DCT1 reading frame [14]. This resulted in the substitutions G50M, S573T, and V574S, which did not change the properties of DCT1. The mutation was confirmed by sequence analysis. The cRNAs of DCT1 and the mutants were synthesized by *in vitro* transcription from their cDNAs. Oocytes were injected with 50 µl water containing 50 ng cRNA.

2.2. Oocyte preparation and uptake measurements

Xenopus laevis oocytes were handled as previously described [14]. Uptake experiments were performed 3 days after injections. The uptake solution for radiotracer experiments contained 100 mM NaCl, 10 mM HEPES, 2 mM MES, 2 mM KCl, 1 mM $CaCl_2$, 1 mM $MgCl_2$, and 2 mM L-ascorbic acid; the pH was adjusted to 7.5 with Tris base (the levels of Tris that were used were low enough to have minimal effects via metal ion binding). Usually, 20 oocytes were incubated in 0.5 ml of a solution containing $^{55}FeCl_2$, $^{54}MnCl_2$, $^{65}ZnCl_2$, or $^{60}CoCl_2$. The

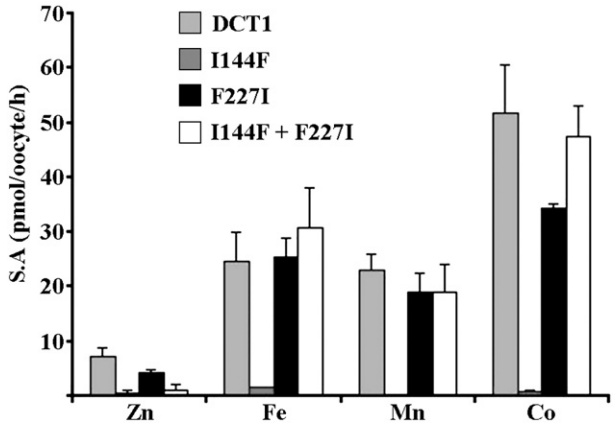

Fig. 2. Uptake of metal ions by *X. laevis* oocytes expressing DCT1 and the mutants I144F, F227I, and I144F/F227I. The uptake experiment was performed at pH 5.5 in solution containing 100 mM NaCl, 2 mM KCl, 1 mM $MgCl_2$, 1 mM $CaCl_2$, 10 mM HEPES, 2 mM MES, 2 mM ascorbic acid, and the indicated metal ion in its chloride form at 7 μM. Each bar represents the mean (after subtraction of the control values)±SEM (n=20). SA, specific activity.

radioactive tracer was mixed with 7 μM unlabeled metal ion, and uptake was assessed for 30 min. The reported values are background-corrected and expressed as specific activity (pmol/oocyte/h).

2.3. Electrophysiological experiments

Two-microelectrode voltage clamp recordings were performed and the data were analyzed as described previously [14,30–32]. To analyze pre-steady state currents, the current traces were fitted to $I(t)=I_1 \exp(-t/\tau_1)+I_2 \exp(-t/\tau_2)+I_{ss}$, where I_1 is a capacitative current with time constant τ_1 associated with the oocyte plasma membrane (τ_1 is also observed in uninjected control oocytes), I_2 is a transient current associated with DCT1 expression with time constant ô$_2$, and I_{ss} is the steady state current. The parameters τ_1, τ_2, I_1, I_2, and I_{ss} were allowed to vary. The transient charge movements Q were obtained from the time integrals of $I_{transient}(t)=I_2 \exp(-t/\tau_2)$ during the off responses for all depolarizing potentials and fitted with the Boltzmann equation, $Q=Q_{max}/\{1+\exp[(V-V_{0.5})zF/RT]\}$, where Q_{max} represents the total charge movement, z represents the effective valence, and $V_{0.5}$ represents the midpoint of the charge distribution [30 31]. *R, T,* and *F* are the usual thermodynamic constants.

3. Results

The two homolog proteins, mammalian DCT1 and yeast Smf1p function as general divalent metal ion transporters. Both use proton gradients as their motive force and exhibit similar affinities for various metal ion substrates [9,14]. Despite their relatively high homology (28% identity), there are a few known differences between DCT1 and Smf1p. The most prominent difference is in transporter slip; H^+ slips through DCT1 and Na^+ slips through Smf1p [13]. These differences must be due to unconserved amino acids in both proteins. Thus, to locate the transporter sites generating ion slip, we substituted amino acids in DCT1 for the corresponding amino acids in Smf1p [12]. Substitution of phenylalanine in position 227 in TM4 of DCT1 (Fig. 1) for the reciprocal isoleucine of Smf1p nearly abolished proton slip without significantly affecting metal ion transport activity (except for a small decrease in Zn^{2+} and Co^{2+} uptake activity) or levels of transporter expression [10].

Noncovalent interactions involving aromatic rings are essential to protein–ligand recognition (including transitional metal ions and protons) and to establishment of protein structure [33–40]. Based on the assumption that phenylalanine residues may be important to the mechanism of these two transporters, we searched for a phenylalanine residue that is present in Smf1p but not in DCT1. We mutated isoleucine-144 of DCT1 (Fig. 1), located in TM2, to the corresponding phenylalanine residue of Smf1p. We then analyzed the properties of the mutant by expression in *Xenopus* oocytes, measurements of uptake activity and recording electrophysiological parameters.

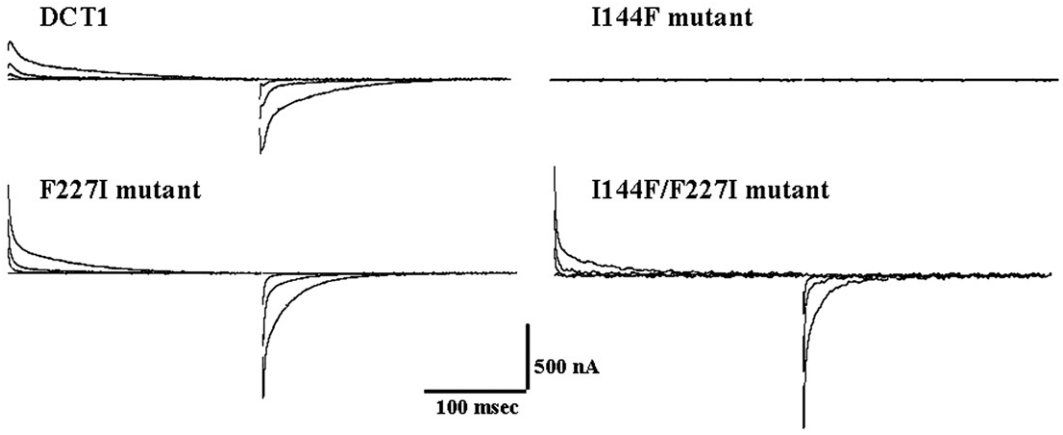

Fig. 3. Pre-steady state charge movements of DCT1 and the mutants I144F, F227I, and I144F/F227I. DCT1 and mutant transporters were expressed in *X. laevis* oocytes, and currents were recorded in a solution containing 100 mM NaCl, 2 mM KCl, 1 mM $MgCl_2$, 1 mM $CaCl_2$, 10 mM HEPES and 2 mM MES. The membrane potential was held at −25 mV and transiently (500 ms) stepped to imposed potentials between +50 mV and −125 mV with 25 mV intervals. Transient currents are plotted against time. The pre-steady state transient currents were obtained from the total currents by subtracting the capacitative and steady state currents. The transient currents were integrated to obtain the charge, and the charge-voltage relations were fitted to the Boltzmann equation (materials and methods). Control oocytes did not exhibit pre-steady state currents. The Boltzmann parameters extrapolated from the fit for DCT1, F227I, and I144F/F227I were: Q_{max}, 36, 32, and 33 nC; $V_{0.5}$, 49, 46, and 51 mV; z, 2, 1.9, 1.8. The time constant ô for the decay of the pre-steady state current with the jump in potential to +50 mV was 64 ms (DCT1) and 22 ms (double mutant) for the on response and 40 ms (DCT1) and 13 ms (double mutant) for the off response.

3.1. Metal Ion Uptake Activity of DCT1 and a I144F Mutant

The uptake activity of Zn^{2+}, Fe^{2+}, Mn^{2+}, and Co^{2+} in *Xenopus* oocytes injected with cRNA of DCT1 or the I144F mutant is shown in Fig. 2. The data are representative of at least three experiments with oocytes from different frogs. The 1144F mutation nearly abolished the transporter's uptake activity at pH 5.5 (Fig. 2) as well as pH 6.5 (data not shown).

3.2. Pre-steady state currents and metal ion-induced steady state currents in oocytes expressing DCT1 and the I144F mutant

At pH 5.5 and a millisecond time scale, oocytes expressing DCT1 exhibited pre-steady state currents, mainly at positively imposed potentials [9,12] (Fig 3A). Pre-steady state currents are an excellent indication of the level of transporter expression in *Xenopus* oocytes [41]. With the addition of metal ion, pre-steady

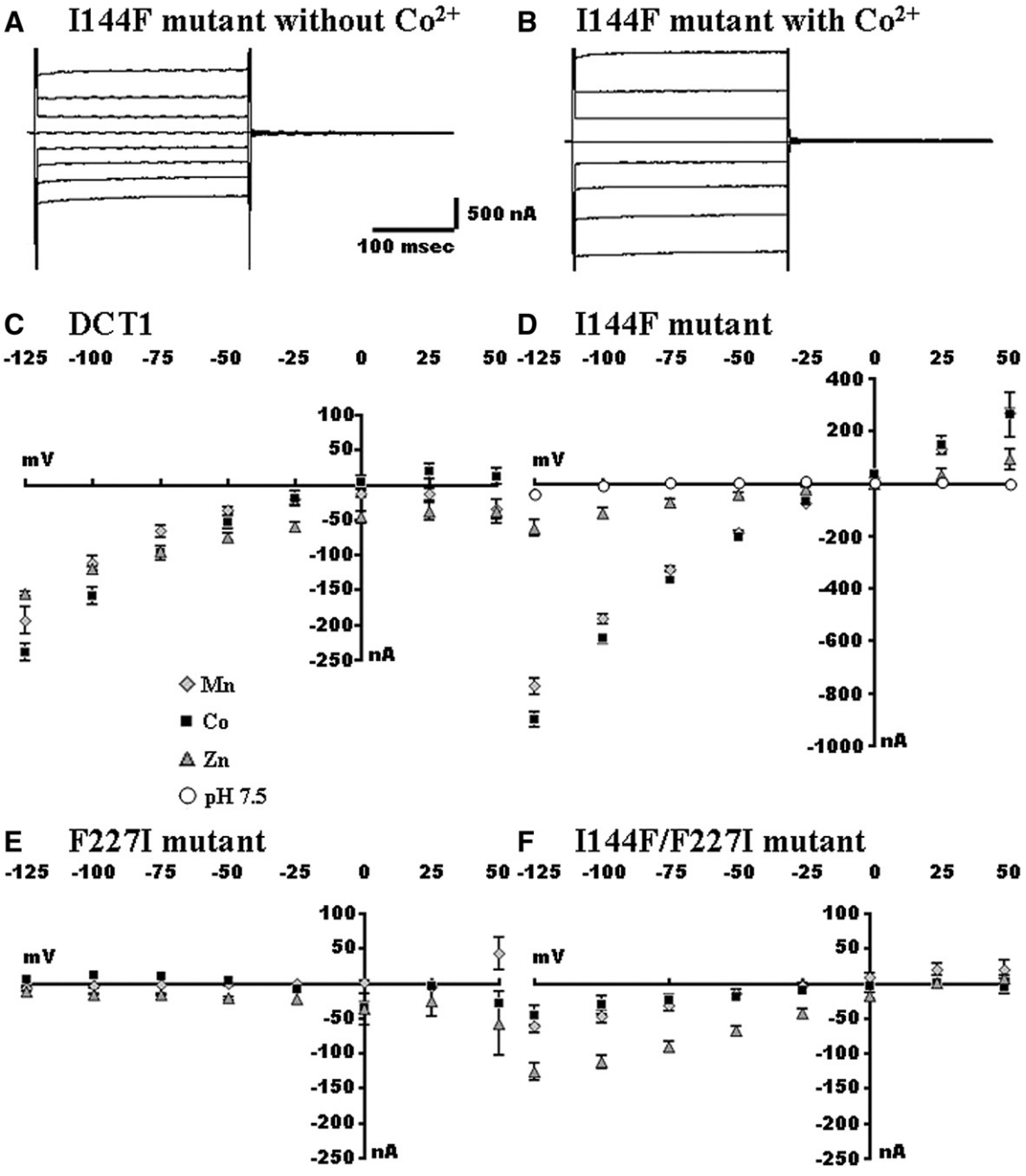

Fig. 4. The effect of Co^{2+} on the steady-state currents in the I144F mutant (A and B). The experiment was performed as described in Fig. 3, with (B) or without (A) 0.1 mM Co^{2+}. The transient currents are plotted against time. Effect of imposed potential on the steady-state currents induced by Zn^{2+}, Mn^{2+}, and Co^{2+} (C–F). The experiment was performed at pH 5.5 in the presence or absence of 0.1 mM $ZnCl_2$ (triangles), $MnCl_2$ (diamonds), or $CoCl_2$ (squares—pH 5.5 and circles—pH 7.5). Steady state substrate-induced currents (in the presence and absence of metal ion) were recorded at each voltage and plotted as a function of V. Each point represents the mean ± SEM (n = 4).

state currents disappeared and large steady state currents appeared, especially at negatively imposed potentials. In contrast, pre-steady state currents were absent in oocytes injected with cRNA of the mutant I144F (Figs. 3B and 4A, the absence of pre-steady-state current in Fig. 3B can be seen from the current records in Fig. 4A). Lack of transport and pre-steady state activities indicates that the transporter was inactivated or failed to assemble in the plasma membrane. Surprisingly, without exception (four independent mRNA injections), addition of metal ion induced steady state currents that were up to 4.5-fold larger then those of native DCT1 (Figs. 4A–D and 5D). Fig. 4C and D shows the metal ion-induced currents generated in oocytes expressing DCT1 and its I144F mutant at different imposed potentials. At −125 mV, addition of 0.1 mM Co^{2+} or Mn^{2+} induced currents of 901±28 nA and 775±33 nA for the I144F mutant and only 239±12 nA and 193±19 nA for DCT1. In contrast, addition of Zn^{2+} induced similar currents of 168±30 nA for the I144F mutant and 156±3 nA for DCT1. The same phenomenon was also observed at induced potentials between −25 mV and −125 mV.

The large positive metal ion-induced currents in DCT1-expressing oocytes at a high proton concentration (pH 5.5) and negative membrane potentials are mainly due to proton movement across the membrane [9,11]. Oocytes expressing the I144F mutant were more sensitive to the presence of Na^+ in the solution than were oocytes expressing native DCT1 (Fig. 5A and B). At −125 mV, exclusion of Na^+ (replacing 100 mM NaCl with choline-Cl) led to a 50% decrease in Co^{2+}-induced currents in oocytes expressing the I144F mutant (Fig. 5B) and a 20% decrease for oocytes expressing DCT1 (Fig. 5A). The difference between mutant and native transporter was more prominent at less negative potentials; at −50 mV, exclusion of Na^+ reduced the currents by 47% for the I144F mutant, without affecting currents for DCT1 (Fig. 5A and B). In contrast to what was found for oocytes expressing native DCT1, the magnitude of Co^{2+}-induced currents in oocytes expressing the I144F mutant was dependent on the Na^+ concentration (Fig. 5D). The currents did not saturate at Na^+ concentrations up to 100 mM at any V_m tested (up to 125 mV) (Fig. 5D). A similar phenomenon was observed for Mn^{2+}-induced currents (data not shown). This suggests that Na^+ transport is part of the large positive inward currents generated by the mutated transporter (sodium slip).

Similar properties of Na^+-dependent unsaturated Na^+ slip were previously described for Smf1p, except that no proton slip

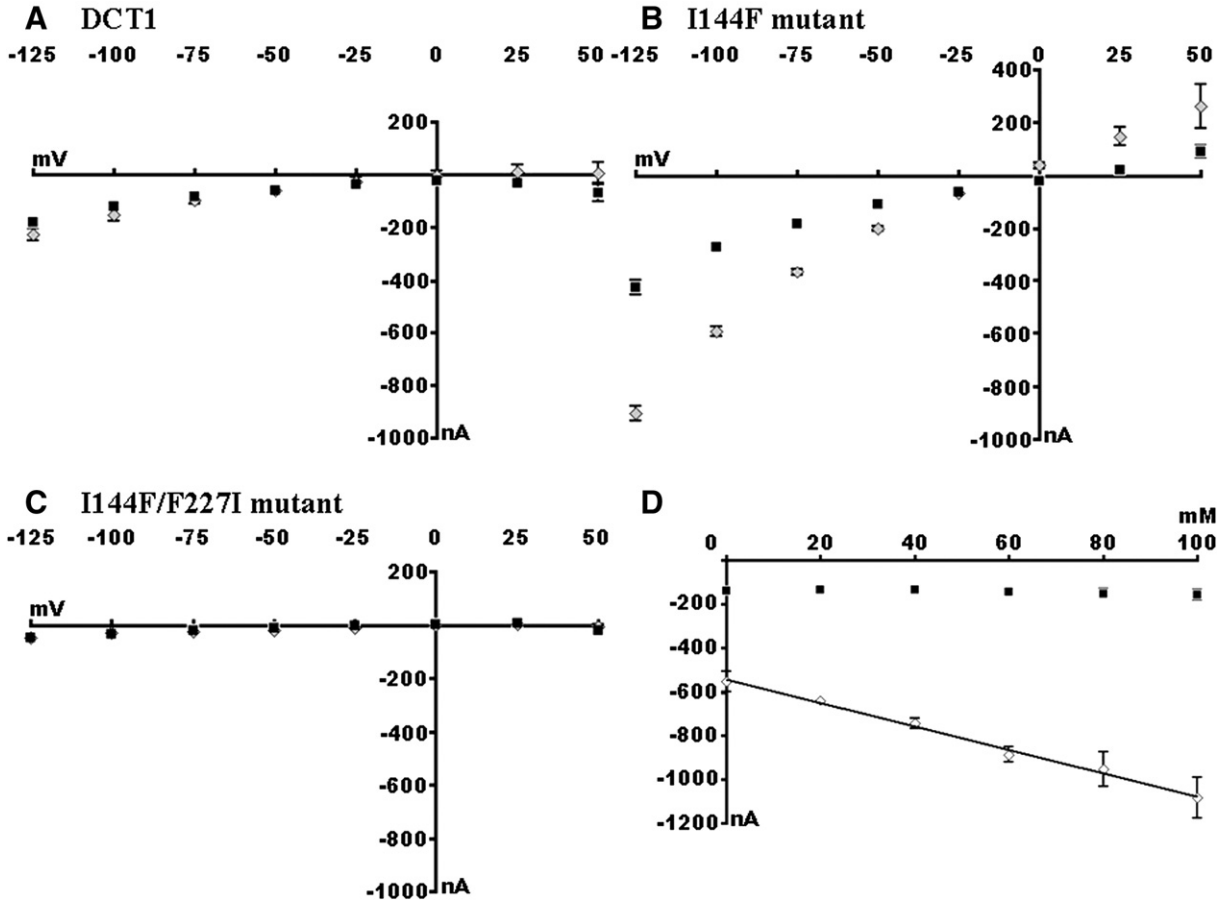

Fig. 5. Effect of Na^+ on Co^{2+}-induced currents at different imposed potentials. The experiment was performed as described for Fig. 3, in the presence of 100 mM NaCl or choline-Cl. Steady state Co^{2+}-induced currents (in the presence and absence of Co^{2+}) were recorded for each voltage in the presence (diamonds) and absence (squares) of Na^+ and plotted as a function of V. (A) DCT1. (B) I144F mutant. (C) I144F/F227I mutant. Each point represents the mean±SEM (n=4). (D) Na^+ concentration-dependence of the currents evoked by 0.1 mM Co^{2+} at V_m=−125 mV and pH_o 5.5 (squares, DCT1; diamonds, I144F mutant; R^2= 0.99, slope=5.35 nA/mM Na^+; n=3).

was detected, and the currents were metal ion-independent [11]. Also, in contrast to what was described for Smf1p, the slip currents for the I144F mutant disappeared at pH 7.5 (Fig. 4D). These results demonstrate the importance of position 144 in the ion translocation pathway of DCT1 and in the mechanism underlying slip.

Mutations F227I and I144F produced opposing effects. The F227I mutation decreased the slip current without affecting the uptake activity of the transporter ([10], Figs. 2 and 4E), while the I144F mutation increased the slip currents and eliminated uptake activity (Figs. 2 and 4D).

3.3. Metal ion uptake activity of the double mutant I144F/F227I

The logical next step was to generate and evaluate a F227I/I144F double mutant. The uptake activity of Zn^{2+}, Fe^{2+}, Mn^{2+}, and Co^{2+} in *Xenopus* oocytes injected with cRNA of the I144F/F227I mutant is shown in Fig. 2. As mentioned above, the mutation I144F in TM2 (Fig. 1) abolished the uptake activity of the transporter. However, elimination of an aromatic ring (I144F/F227I) located two trans membrane domains after TM2 (TM4, Fig. 1) restored uptake of Fe^{2+}, Mn^{2+}, and Co^{2+} without affecting the low level of Zn^{2+} uptake present with the I144F mutant (Fig. 2). These results suggest proximity of these two positions (144 and 227) in the folded structure of DCT1 and support the importance of position 144 in metal ion transport.

3.4. Pre-steady state currents in the double mutant I144F/F227I

As mentioned above, unlike DCT1, the mutant I144F did not exhibit pre-steady state currents (Fig. 3A and B). As we previously reported [10], the F227I mutation did not significantly affect the pre-steady state currents of DCT1. However, the F227I mutation suppressed the effect of the I144F mutation, restoring not only metal ion uptake activity (Fig. 2) but also the pre-steady state currents (Fig. 3D). The magnitude of the pre-steady state currents recorded in oocytes expressing native DCT1, the F227I mutant, or the double mutant I144F/F227I (Fig. 3A, B, and D) indicated similar levels of expression of the three transporters. To characterize the features of the I144F/F227I mutant, we subtracted the capacitative and steady state currents to yield the transient current (Q) (Fig. 3D). At each applied voltage, time integration of the off transients yielded the charge moved. The charge–voltage (Q–V) relationship obtained (data not shown) was fitted to a single Boltzmann function. Similar Q_{max} of 36, 32, and 33 nC, similar $V_{0.5}$ of 49, 46, and 51 mV, and similar z values of 2, 1.9 and 1.8 were extrapolated from the fit for DCT1, F227I, and I144F/F227I, respectively. The time constant ô for the pre-steady state current decay for I144F/F227I, with a jump in potential from −25 mV to +50 mV, was 22 ms for the on response and 13 ms for the off response, whereas for DCT1, τ was 64 ms and 40 ms for the on and off response, respectively. According to the Q_{max}, $\sim 2\times10^{11}$ transporters were expressed on the plasma membrane of each oocyte expressing DCT1, the F227I mutant, or the I144F/F227I mutant. This calculation was made based on the mechanistic concept of transient charge movements in ion-coupled transporters proposed by Wright and coworkers [30,42] for the Na^+-coupled glucose transporter SGLT1 and considering the similarity between the pre-steady state properties of SGLT1 and DCT1. Essentially, the pre-steady state current results from imposed potential induction of occlusion and release of protons by DCT1 in the absence of substrate [1]. The decrease in ô for the double mutant I144F/F227I might indicate increased accessibility of protons to their binding sites on the mutated transporter.

3.5. Metal Ion-Induced Steady State Currents in the Double Mutant I144F/F227I

Addition of Mn^{2+} or Co^{2+} to oocytes expressing the I144F/F227I mutant resulted in the disappearance of the pre-steady state currents and appearance of steady state currents smaller than those observed for native DCT1 (Fig. 4F). At −125 mV, addition of Mn^{2+} or Co^{2+} induced inward positive currents of 193±19 nA or 239±12 nA for DCT1 (Fig. 4C) and 60±10 nA or 46±14 nA for the I144F/F227I mutant (Fig. 4F). Addition of Zn^{2+} abolished pre-steady state currents in oocytes expressing the double mutant but induced similar currents of 156±3 nA and 127±12 nA for DCT1 and the I144F/F227I mutant, respectively. The double mutant partially retained the properties of the F227I mutant (Fig 4E), exhibiting reduced slip currents with Mn^{2+} and Co^{2+}, and retained the response of I144F to Zn^{2+} (Fig 4F). Metal ion-induced currents of the double mutant were not influenced by the presence or absence of Na^+ in the solution (Fig. 5C).

The functional properties of the two mutations encoded by the mutated *DCT1* gene in the most recently reported human patient with congenital hypochromic microcytic anemia (in-frame deletion of V145 and G243V) are unknown [28]. This patient is a compound heterozygote for the two mutations in *DCT1*. The prominent effects of the I144F mutation located immediately before V145 demonstrate the transporter's sensitivity to alterations in this region. It is probable that deletion of V145 severely impairs transporter activity.

4. Discussion

The advantage of precision in biological processes is obvious. However, in many cases, deviations from faithful mechanisms occur. The terms "slips" and "leaks" have been used to describe deviation from the expected stoichiometry of an operating system [43–46]. We use the term slip to describe a built-in feature of a specific protein or complex and the term leak to describe a general property of the membrane, that is, summation of the membrane's permeability.

DCT1 and Smf1p are quintessential examples of transporters that generate a built-in slip current as part of their mechanism of action. In both DCT1 and Smf1p transporters, protons are the driving force for metal ion uptake [9,12–14]. Under conditions of neutral pH and/or neutral membrane potential, DCT1 is in the coupled state; the stoichiometry of proton: metal ion transport is close to 1:1. Increasing the driving force by reducing the pH or increasing the negative potential generates a proton slip, which

maintains the levels of substrate transport at rates that are close to the normal rates for the coupled state. However, slip significantly increases the rate of proton movement through the transporter. A similar mechanism applies to Smf1p-mediated slip, except that Na^+ slips rather than H^+. Na^+ inhibits the metal ion uptake by Smf1P [11,14]. The physiological significance of this phenomenon may be that it protects cells against excessive transport of these elements. Such a mechanism is necessary when cells are exposed to conditions of abundant metals and an acidic environment. We propose that slips are fundamental to life processes, enabling cells to cope with stressful situations created by transitory extreme conditions, which might otherwise impair cell functioning and jeopardize its health. However, the mechanism underlying H^+ and Na^+ slip in metal ion transporters is unclear.

To locate the transporter sites that generate slip, we used reciprocal amino acid substitution between DCT1 and Smf1p to manipulate slip magnitude and ion composition. Substitution of a single amino acid in F227I in TM4 reduced proton slip through DCT1 without significantly affecting metal ion transport [10]. This mutation did not generate Na^+ slip, and the transporter properties were unaffected by removal of Na^+ from the bathing medium [10]. However, mutation I144F in TM2 increased slip currents induced by Co^{2+} and Mn^{2+} (but not Zn^{2+}) and eliminated the transporter's metal ion transport activity (Fig. 2 and 4D). In the presence of metal ions, there was charge slip, but the metal ion was not transported across the membrane. In addition to the proton slip mutation I144F of DCT1 also produced Na^+ slip (Fig. 5). The loss of metal ion transport ability with this mutation could be explained by the increase in slip currents. However, reduction of proton concentration or omission of Na^+ did not increase uptake activity (data not shown). These results demonstrate the importance of position 144 to metal ion transport, ion permeability, and ion selectivity. It appears that this position participates in formation of the translocation pathway in DCT1 and Smf1p, and it is probably one of the sites responsible for generating sodium slip in Smf1p.

The mutation I144F did not generate any pre-steady state currents. This could be due to changes in the proton-binding site of the transporter; according to the mechanistic concept of transient charge movements [30,42], the pre-steady state current results from occlusion and release of protons by DCT1 in response to imposed membrane potential in the absence of substrate. We propose that this position also participates in the formation of the proton-binding site of DCT1. The F227I substitution in the I144F mutant (I144F/F227I) suppressed the effect of the I144F mutation, restored its metal ion uptake (Fe^{2+}, Co^{2+}, and Mn^{2+} but not Zn^{2+}) and pre-steady state currents, and reduced metal ion-induced (Co^{2+} and Mn^{2+} but not Zn^{2+}) slip currents to a level below that for native DCT1 (Figs. 2, 3D and 4D). This substitution might restore the environment of the proton-binding site and the metal ion translocation pathway to their state in native DCT1, thus enabling pre-steady state currents and metal ion uptake. These findings suggest that position 144 in TM2 and position 227 in TM4 are located in close proximity within the folded structure of DCT1.

Differences in Zn^{2+} transport and Zn^{2+}-induced steady state currents for the various mutations are noteworthy. The F227I mutant transported Zn^{2+} and produced smaller steady state currents than those observed for native DCT1, thus increasing the coupling between Zn^{2+} and protons ([10], Figs. 2 and 4E). The I144F mutant did not transport Zn^{2+} or any other metal ion tested; also, it increased the steady state currents induced by Mn^{2+} and Co^{2+} but not Zn^{2+} (Figs. 2 and 4D). The double mutant I144F/F227I transported Mn^{2+} and Co^{2+}, but not Zn^{2+}, and did not reduce Zn^{2+}-induced steady state currents, an indication that the double mutation does not increase coupling between Zn^{2+} and protons (Figs. 2 and 4D). Therefore, this region of DCT1 is likely involved in the transporter's metal ion and proton coupling, and metal ion specificity. Further studies will be required to identify the binding sites and the translocation pathway that was influenced by the I144F and F227I mutations in DCT1.

Our findings suggest that aromatic residues in DCT1, and probably in other family members, play an important mechanistic role. Previous studies have established the importance of aromatic residues to protein–ligand recognition (including transitional metal ions and protons) and the establishment of protein structure [33–40]. Cation–pi interactions are common among structures in the Protein Data Bank, and it is clear that the presence of a cationic residue (Lys or Arg) near an aromatic residue (Phe, Tyr, or Trp) biases the geometry so as to promote a favorable cation–pi interaction [34]. The Arg residue is more likely than Lys to participate in a cation–pi interaction [34]. The highly conserved arginine reside in position 151 (Fig. 1), seven amino acids after I144, could be located in the same region as I144 and F227, two turns further in an α-helix structure. Substitution of R151 to Y decreased metal ion transport by up to 90% (Sacher, A., unpublished results). Lam-Yuk-Tseung et al. showed that the mutation R151A fully complemented the susceptibility of the yeast smf1/smf2 mutant (where SMF1 and SMF2 genes are insertionally inactivated) to the metal chelator EGTA [22]. However, as we observed from our previous studies, manganese uptake activity of approximately 10% was sufficient to complement the yeast null SMF1 mutant [12]. The R151 residue may participate in a cation–pi interaction with F227 in this region of DCT1. There has been great progress in structure–function analyses of the Nramp family [10,12,15,22,47,48]. However, only a high-resolution structure of one or more family members can confirm these predictions and provide a detailed description of the unusual operating mechanism for this important family of metal ion transporters.

Acknowledgment

I would like to thank my mentor Prof. Nathan Nelson for the guidance, the infinite knowledge and wisdom, and for being such a great man.

References

[1] N. Nelson, Metal ion transporters and homeostasis, EMBO J. 18 (1999) 4361–4371.
[2] J.R. Forbes, P. Gros, Divalent-metal transport by NRAMP proteins at the interface of host–pathogen interactions, Trends Microbiol. 9 (2001) 397–403.
[3] A. Van Ho, D.M. Ward, J. Kaplan, Transition metal transport in yeast, Annu. Rev. Microbiol. 56 (2002) 237–261.

[4] T. Goswami, A. Rolfs, M.A. Hediger, Iron transport: emerging roles in health and disease, Biochem. Cell. Biol. 80 (2002) 679–689.
[5] D. Agranoff, L. Collins, D. Kehres, T. Harrison, M. Maguire, S. Krishna, The Nramp orthologue of *Cryptococcus neoformans* is a pH-dependent transporter of manganese, iron, cobalt and nickel, Biochem. J. 385 (2005) 225–232.
[6] F. Supek, L. Supekova, H. Nelson, N. Nelson, A yeast manganese transporter related to the macrophage protein involved in conferring resistance to mycobacteria, Proc. Natl. Acad. Sci. U. S. A. 93 (1996) 5105–5110.
[7] F. Supek, L. Supekova, H. Nelson, N. Nelson, Function of metal-ion homeostasis in the cell division cycle, mitochondrial protein processing, sensitivity to mycobacterial infection and brain function, J. Exp. Biol. 200 (1997) 321–330.
[8] X.F. Liu, F. Supek, N. Nelson, V.C. Culotta, Negative control of heavy metal uptake by the *Saccharomyces cerevisiae* BSD2 gene, J. Biol. Chem. 272 (1997) 11763–11769.
[9] H. Gunshin, B. Mackenzie, U.V. Berger, Y. Gunshin, M.F. Romero, W.F. Boron, S. Nussberger, J.L. Gollan, M.A. Hediger, Cloning and characterization of a proton-coupled mammalian metal-ion transporter, Nature 388 (1997) 482–488.
[10] Y. Nevo, N. Nelson, The mutation F227I increases the coupling of metal ion transport in DCT1, J. Biol. Chem. 27951 (2004) 53056–53061.
[11] X.Z. Chen, J.B. Peng, A. Cohen, H. Nelson, N. Nelson, M.A. Hediger, Yeast SMF1 mediates H(+)-coupled iron uptake with concomitant uncoupled cation currents, J. Biol. Chem. 274 (1999) 35089–35094.
[12] A. Cohen, Y. Nevo, N. Nelson, The first external loop of the metal-ion transporter DCT1 is involved in metal-ion binding and specificity, Proc. Natl. Acad. Sci. U. S. A. 100 (2003) 10694–10699.
[13] N. Nelson, A. Sacher, H. Nelson, The significance of molecular slips in transport systems, Nat. Rev., Mol. Cell Biol. 3 (2002) 876–881.
[14] A. Sacher, A. Cohen, N. Nelson, Properties of the mammalian and yeast metal-ion transporters DCT1 and Smf1p expressed in *Xenopus laevis* oocytes, J. Exp. Biol. 2046 (2001) 1053–1061.
[15] Y. Nevo, N. Nelson, The NRAMP family of metal-ion transporters, Biochim. Biophys. Acta 763 (2006) 609–620.
[16] N.C. Andrews, Iron homeostasis: insights from genetics and animal models, Nat. Rev., Genet. 1 (2000) 208–217.
[17] M. Wessling-Resnick, Iron transport, Annu. Rev. Nutr. 20 (2000) 129–151.
[18] H. Gunshin, Y. Fujiwara, A.O. Custodio, C. DiRenzo, S. Robine, N.C. Andrews, Slc11a2 is required for intestinal iron absorption and erythropoiesis but dispensable in placenta and liver, J. Clin. Invest. 115 (2005) 1258–1266.
[19] M.D. Fleming, M.A. Romano, M.A. Su, L.M. Garrick, M.D. Garrick, N.C. Andrews, Nramp2 is mutated in the anemic Belgrade (b) rat: evidence of a role for Nramp2 in endosomal iron transport, Proc. Natl. Acad. Sci. U. S. A. 95 (1998) 1148–1153.
[20] M.D. Fleming, C.C. Trenor, M.A. Su, D. Foernzler, D.R. Beier, W.F. Dietrich, N.C. Andrews, Microcytic anaemia mice have a mutation in *Nramp2*, a candidate iron transporter gene, Nat. Genet. 16 (1997) 383–386.
[21] F. Canonne-Hergaux, A.S. Zhang, P. Ponka, P. Gros, Characterization of the iron transporter DMT1 (NRAMP2/DCT1) in red blood cells of normal and anemic *mk/mk* mice, Blood 98 (2001) 3823–3830.
[22] S. Lam-Yuk-Tseung, G. Govoni, P. Gros, Iron transport by NRAMP2/DMT1: pH regulation of transport by two histidines in transmembrane domain 6, Blood 101 (2003) 3699–3707.
[23] S. Lam-Yuk-Tseung, M. Mathieu, P. Gros, Functional characterization of the E399D DMT1/NRAMP2/SLC11A2 protein produced by an exon 12 mutation in a patient with microcytic anemia and iron overload, Blood Cells Mol. Diseases 352 (2005) 212–216.
[24] M.P. Mims, Y. Guan, D. Pospisilova, M. Priwitzerova, K. Indrak, P. Ponka, V. Divoky, J.T. Prchal, Identification of a human mutation of DMT1 in a patient with microcytic anemia and iron overload, Blood 105 (2005) 1337–1342.
[25] H. Gunshin, J. Jin, Y. Fujiwara, N.C. Andrews, M. Mims, J. Prchal, Analysis of the E399D mutation in SLC11A2, Blood 106 (2005) 2221–2222.
[26] M. Priwitzerova, G. Nie, A.D. Sheftel, D. Pospisilova, V. Divoky, P. Ponka, Functional consequences of the human DMT1 (SLC11A2) mutation on protein expression and iron uptake, Blood 106 (2005) 3985–3987.
[27] A. Iolascon, M. d'Apolito, V. Servedio, F. Cimmino, A. Piga, C. Camaschella, Microcytic anemia and hepatic iron overload in a child with compound heterozygous mutations in DMT1 (SCL11A2), Blood 107 (2006) 349–354.
[28] C. Beaumont, J. Delaunay, G. Hetet, B. Grandchamp, M. de Montalembert, G. Tchernia, Two new human DMT1 gene mutations in a patient with microcytic anemia, low ferritinemia, and liver iron overload, Blood 107 (2006) 4168–4170.
[29] T. Noumi, C. Beltrán, H. Nelson, N. Nelson, Mutational analysis of yeast vacuolar H(+)-ATPase, Proc. Natl. Acad. Sci. U. S. A. 88 (1991) 1938–1942.
[30] D.D. Loo, A. Hazama, S. Supplisson, E. Turk, E.M. Wright, Relaxation kinetics of the Na^+/glucose cotransporter, Proc. Natl. Acad. Sci. U. S. A. 90 (1993) 5767–5771.
[31] D.D. Loo, B.A. Hirayama, E.M. Gallardo, J.T. Lam, E. Turk, E.M. Wright, Conformational changes couple Na^+ and glucose transport, Proc. Natl. Acad. Sci. U. S. A. 95 (1998) 7789–7794.
[32] X.-Z. Chen, C. Shayakul, U.V. Berger, W. Tian, M.A. Hediger, Characterization of a rat Na^+-dicarboxylate cotransporter, J. Biol. Chem. 273 (1998) 20972–20981.
[33] E.A. Meyer, R.K. Castellano, F. Diederich, Interactions with aromatic rings in chemical and biological recognition, Angew. Chem., Int. Ed. 42 (2003) 1210–1250.
[34] J.P. Gallivan, D.A. Dougherty, Cation–pi interactions in structural biology, Proc. Natl. Acad. Sci. U. S. A. 96 (1999) 9459–9464.
[35] R.A. Srinivas, S.G. Narahari, LE-like erythema and periungual telangiectasia among coffee plantation workers, J. Phys. Chem. 109 (2005) 8893–8903.
[36] A. Rimola, L. Rodriguez-Santiago, M.J. Sodupe, Cation–pi Interactions and oxidative effects on Cu^+ and Cu^{2+} binding to Phe, Tyr, Trp, and His amino acids in the gas phase. Insights from first-principles calculations, Phys. Chem. B 110 (2006) 24189–24199.
[37] N.C. Polfer, J. Oomens, D.T. Moore, G. von Helden, G. Meijer, R.C. Dunbar, Infrared spectroscopy of phenylalanine Ag(I) and Zn(II) complexes in the gas phase, J. Am. Chem. Soc. 128 (2006) 517–525.
[38] H. Takeuchi, A. Okada, T. Miura, Roles of the histidine and tryptophan side chains in the M2 proton channel from influenza A virus, FEBS Lett. 552 (2003) 35–38.
[39] R. Wintjens, C. Noel, A.C. May, D. Gerbod, F. Dufernez, M. Capron, E. Viscogliosi, M. Rooman, Specificity and phenetic relationships of iron- and manganese-containing superoxide dismutases on the basis of structure and sequence comparisons, J. Biol. Chem. 279 (2004) 9248–9254.
[40] M.K. Gilson, T.P. Straatsma, J.A. McCammon, D.R. Ripoll, C.H. Faerman, P.H. Axelsen, I. Silman, J.L. Sussman, Open "back door" in a molecular dynamics simulation of acetylcholinesterase, Science 263 (1994) 1276–1278.
[41] E.M. Wright, D.D. Loo, M. Panayotova-Heiermann, M.P. Lostao, B.H. Hirayama, B. Mackenzie, K. Boorer, G. Zampighi, 'Active' sugar transport in eukaryotes, J. Exp. Biol. 196 (1994) 197–212.
[42] B. Mackenzie, D.D. Loo, Y. Fei, W. Liu, V. Ganapathy, F.H. Leibach, E.M. Wright, Mechanisms of the human intestinal H^+-coupled oligopeptide transporter hPEPT1, J. Biol. Chem. 271 (1996) 5430–5437.
[43] D. Pietrobon, M. Zoratti, G.F. Azzone, S.R. Caplan, Intrinsic uncoupling of mitochondrial proton pumps. 2. Modeling studies, Biochemistry 25 (1986) 767–775.
[44] S.R. Caplan, The contribution of intrinsic uncoupling ("slip") to the regulation of ion pumps, in particular bacteriorhodopsin, Prog. Clin. Biol. Res. 273 (1988) 377–386.
[45] K. Van Dam, Regulation and control of energy coupling at the cellular level, Biochim. Biophys. Acta 1187 (1994) 129–131.
[46] S. Schuster, H.V. Westerhoff, Modular control analysis of slipping enzymes, Biosystems 49 (1999) 1–15.
[47] R. Chaloupka, P. Courville, F. Veyrier, B. Knudsen, T.A. Tompkins, M.F. Cellier, Identification of functional amino acids in the Nramp family by a combination of evolutionary analysis and biophysical studies of metal and proton cotransport in vivo, Biochemistry 44 (2005) 726–733.
[48] P. Courville, R. Chaloupka, M.F. Cellier, Recent progress in structure–function analyses of Nramp proton-dependent metal-ion transporters, Biochem. Cell. Biol. 84 (2006) 960–978.